

Deeply Bound Kaonic Clusters

E. Oset^{1,a}, V. K. Magas², A. Ramos², S. Hirenzaki³, J. Yamagata-Sekihara^{1,4}, A. Martinez Torres¹, K. P. Khemchandani⁵, M. Napsuciale⁶, L.S. Geng¹, and D. Gamermann¹

¹ Departamento de Física Teórica and IFIC, Centro Mixto Universidad de Valencia-CSIC, 46100 Burjassot (Valencia), Spain

² Departament d'Estructura i Constituents de la Matèria, Universitat de Barcelona, Diagonal 647, 08028 Barcelona, Spain

³ Department of Physics, Nara Women's University, Nara 630-8506, Japan

⁴ Yukawa Institute for Theoretical Physics, Kyoto University, Kyoto 606-8502, Japan

⁵ Centro de Física Teórica, Departamento de Física, Universidade de Coimbra, P-3004-516 Coimbra, Portugal

⁶ Departamento de Física, División de Ciencias e Ingenierías, Universidad de Guanajuato, Campus León, Lomas del Bosque 103, Fraccionamiento Lomas del Campestre, 37150, León, Guanajuato, México.

Abstract In this talk I make a review on the theoretical and experimental situation around the deeply bound kaon clusters, the possible bound kaonic states of nuclear, rather than atomic nature. At the same time I discuss novel developments around other kind of bound kaon clusters, which include states of two mesons and one baryon, with either one or two kaons, and states of a vector meson and two kaons, which explain naturally the observed properties of the X(2175) and Y(4260) resonances.

1 Introduction

In this talk I will review the present situation around the deeply bound kaonic states. The negative kaons experience an attraction in nuclear matter, which has been proved experimentally by the observation of shifts in energy of the kaonic atoms levels. For these kaonic states the Coulomb interaction and the strong one participate on equal footing, but the strength of the strong attraction is found to be large enough to accommodate bound states of nuclear type, where the radius of the kaon is similar to that of the nucleons. The question arises that at the same time the kaon finds modes of annihilation in the presence of other nucleons and the widths of these states can be much larger than the separation between the levels, in which case the possibility to find peaks experimentally fades away. This seems to be the case according to calculations made using chiral dynamical models. Yet, this has not precluded the experimental search for such states and in several experiments claims have been made for their finding. Unfortunately, the claims were based on misinterpretation of peaks, that devoted works, simulating the experiments and the reactions taking place there, have shown could be reproduced in term of conventional, unavoidable reactions occurring in the experiment. Work follows in different laboratories looking for other signals and for the lightest of all these clusters, the $\bar{K}NN$ system.

I also devote some time to describe new systems, which have been studied very recently, and which involve other

kind of clusters of kaons. These states, however, are not controversial. Some of them correspond to states already known, offering a particular interpretation of their nature, and others are predictions for which there could be already some experimental evidence, but which require more work to be settled. The known states to which I refer are the low lying excited $1/2^+$, $S=-1$ resonances, which appear naturally as bound states or resonances of systems of two mesons and one baryon in coupled channels, one of the mesons being a kaon. Another state, which is claimed to be seen in the $\gamma p \rightarrow K^+ \Lambda$ reaction around 1920 MeV, corresponds to a bound state of $K\bar{K}N$ with the K and \bar{K} coupled to make the $f_0(980)$ or $a_0(980)$ resonance. Finally, two more states recently found at BABAR and other labs, the X(2175) and Y(4260), are shown to be well reproduced as resonances of the $\phi K\bar{K}$ and $J/\psi K\bar{K}$ systems respectively. These three body systems have all been studied with a novel approach to the Faddeev equations in coupled channels, using chiral unitary dynamics and the on-shell two body amplitudes, after the useful finding that there is a cancellation of off-shell parts of the two body amplitudes with the three body amplitudes originated by the same chiral Lagrangians. This finding is relevant since it allows one to use empirical amplitudes to solve these Faddeev equations without resorting to the use of potentials and their unavoidable off-shell extrapolation. It also has practical simplifying consequences in the solution of the Faddeev equations that will be discussed.

In the next two sections we study the basic KN interaction using chiral dynamics and the chiral unitary approach in coupled channels. In the two following sections

^a e-mail: oset@ific.uv.es

we study the kaons in a nuclear medium and review the situation of the deeply bound kaon states. A more detailed study is made of one of the reactions claimed to provide evidence of a deeply bound kaon cluster from correlated Λd pairs emitted after the absorption of kaons at rest in nuclei. The $\bar{K}NN$ system is reviewed in another section and in a further section we study the novel three body systems which lead to the interesting states mentioned above.

2 Meson-nucleon amplitudes to lowest order

Following [1,2] we write the lowest order chiral Lagrangian, coupling the octet of pseudoscalar mesons to the octet of $1/2^+$ baryons, as

$$L_1^{(B)} = \langle \bar{B} i \gamma^\mu \nabla_\mu B \rangle - M_B \langle \bar{B} B \rangle +$$

$$\frac{1}{2} D \langle \bar{B} \gamma^\mu \gamma_5 \{u_\mu, B\} \rangle + \frac{1}{2} F \langle \bar{B} \gamma^\mu \gamma_5 [u_\mu, B] \rangle, \quad (1)$$

where the symbol $\langle \rangle$ denotes trace of SU(3) matrices and

$$\begin{aligned} \nabla_\mu B &= \partial_\mu B + [\Gamma_\mu, B] \\ \Gamma_\mu &= \frac{1}{2}(u^+ \partial_\mu u + u \partial_\mu u^+) \\ U &= u^2 = \exp(i \sqrt{2} \Phi / f) \\ u_\mu &= i u^+ \partial_\mu U u^+ \end{aligned} \quad (2)$$

The SU(3) matrices for the mesons and the baryons are the following

$$\Phi = \begin{pmatrix} \frac{1}{\sqrt{2}}\pi^0 + \frac{1}{\sqrt{6}}\eta & \pi^+ & K^+ \\ \pi^- & -\frac{1}{\sqrt{2}}\pi^0 + \frac{1}{\sqrt{6}}\eta & K^0 \\ K^- & \bar{K}^0 & -\frac{2}{\sqrt{6}}\eta \end{pmatrix} \quad (3)$$

$$B = \begin{pmatrix} \frac{1}{\sqrt{2}}\Sigma^0 + \frac{1}{\sqrt{6}}\Lambda & \Sigma^+ & p \\ \Sigma^- & -\frac{1}{\sqrt{2}}\Sigma^0 + \frac{1}{\sqrt{6}}\Lambda & n \\ \Xi^- & \Xi^0 & -\frac{2}{\sqrt{6}}\Lambda \end{pmatrix} \quad (4)$$

At lowest order in momentum, that we will keep in our study, the interaction Lagrangian comes from the Γ_μ term in the covariant derivative and we find

$$L_1^{(B)} = \langle \bar{B} i \gamma^\mu \frac{1}{4f^2} [(\Phi \partial_\mu \Phi - \partial_\mu \Phi \Phi) B - B(\Phi \partial_\mu \Phi - \partial_\mu \Phi \Phi)] \rangle \quad (5)$$

which leads to a common structure of the type $\bar{u} \gamma^\mu (k_\mu + k'_\mu) u$ for the different channels, where u, \bar{u} are the Dirac spinors and k, k' the momenta of the incoming and outgoing mesons.

We take the $K^- p$ state and all those that couple to it within the chiral scheme. These states are $\bar{K}^0 n, \pi^0 \Lambda, \pi^0 \Sigma^0, \pi^+ \Sigma^-, \pi^- \Sigma^+, \eta \Lambda, \eta \Sigma^0, K^0 \Xi^0, K^+ \Xi^-$. Hence we have a problem with ten coupled channels. The lowest order amplitudes for these channels are easily evaluated from eq. (5) and are given by

$$V_{ij} = -C_{ij} \frac{1}{4f^2} \bar{u}(p') \gamma^\mu u(p) (k_\mu + k'_\mu) \quad (6)$$

where $p, p'(k, k')$ are the initial, final momenta of the baryons (mesons). Also, for low energies one can safely neglect the spatial components in eq. (6) and only the γ^0 component becomes relevant, hence simplifying eq. (6) which becomes

$$V_{ij} = -C_{ij} \frac{1}{4f^2} (k^0 + k'^0) \quad (7)$$

The matrix C_{ij} , which is symmetric, is given in [3].

3 Coupled channels Bethe Salpeter equations

Following [4] we write the set of Bethe Salpeter equations in the $\bar{K}N$ centre of mass frame

$$T_{ij} = V_{ij} + V_{il} G_l T_{lj} \quad (8)$$

where the indices i, j run over all possible channels. Eqs. (8) are coupled channels integral equations involving the off shell part of V and T. However, by using the N/D method and neglecting the left hand cut, as done in Quantum Mechanics, one can show that a very useful form of these equations is possible, by writing the potential and the T matrix on shell and factorizing them outside the integral involving VGT. A different derivation is provided in [5] starting from a potential in momentum space, which is separable and has a cut off in momentum

$$V(\mathbf{q}, \mathbf{q}') = V \theta(\Lambda - |\mathbf{q}|) \theta(\Lambda - |\mathbf{q}'|) \quad (9)$$

Thus the BS equations result into the algebraic matrix equations

$$T = V + V G T \quad (10)$$

or equivalently

$$T = [1 - V G]^{-1} V \quad (11)$$

with G a diagonal matrix given by

$$\begin{aligned} G_l &= i \int \frac{d^4 q}{(2\pi)^4} \frac{M_l}{E_l(\mathbf{q})} \frac{1}{k^0 + p^0 - q^0 - E_l(\mathbf{q}) + i\epsilon} \frac{1}{q^2 - m_l^2 + i\epsilon} \\ &= \int \frac{d^3 q}{(2\pi)^3} \frac{1}{2\omega_l(q)} \frac{M_l}{E_l(\mathbf{q})} \frac{1}{p^0 + k^0 - \omega_l(\mathbf{q}) - E_l(\mathbf{q}) + i\epsilon} \end{aligned} \quad (12)$$

which is regularized using either dimensional regularization or a cutoff, q_{max} , and depends on $p^0 + k^0 = \sqrt{s}$ and a subtraction constant in dimensional regularization or q_{max} in the cutoff method.

It is interesting to note here, because it will be used later on, that the Lagrangian of eq. (5) has kept only two mesons in the expansion of Γ_μ of eq. (2). One can keep up to four mesons in the expansion and obtain amplitudes for two mesons one baryon going to also two mesons and one baryon, which will be used in the section devoted to three body states.

4 Kaons in a nuclear medium

The model discussed in the former section for the $\bar{K}N$ interaction gives rise to a s-wave \bar{K} self-energy ($\bar{K} = K^-$ or \bar{K}^0)

$$\Pi_{\bar{K}}^s(q^0, \mathbf{q}, \rho) = 2 \int \frac{d^3 p}{(2\pi)^3} n(\mathbf{p}) \left[T_{\text{eff}}^{\bar{K}p}(P^0, \mathbf{P}, \rho) + T_{\text{eff}}^{\bar{K}n}(P^0, \mathbf{P}, \rho) \right], \quad (13)$$

which is obtained by summing the in-medium $\bar{K}N$ interaction, T_{eff}^α ($\alpha = \bar{K}p, \bar{K}n$), over the nucleons in the Fermi sea. The values (q^0, \mathbf{q}) stand now for the energy and momentum of the \bar{K} in the lab frame. Note that a self-consistent approach is required since one calculates the \bar{K} self-energy from the effective interaction T_{eff} which uses \bar{K} propagators which themselves include the self-energy being calculated.

The T matrices in eq. (13) are modified in the medium to take into account Pauli blocking on the intermediate nucleons, pionic selfenergies and kaon selfenergies of the intermediate states. The p-wave contributions coming from the coupling of the \bar{K} meson to hyperon particle-nucleon hole (YN^{-1}) excitations are also taken into account.

The method outlined above has been used in [6,7,8,9] considering Pauli blocking effects. The work of [10] considers the selfenergy of the pions in addition and the self-energy of the kaons selfconsistently. The selfconsistency requirement is mandatory in the presence of the nearby $\Lambda(1405)$ resonance and is also implemented in [9,11,12], where similar results are obtained. The p-waves have been considered in addition in [13].

With this method we obtain a shallow potential which is common to all the chiral approaches including selfconsistency, and which we show in fig. 1.

It is interesting to note that with this potential one could get a good reproduction of shifts and widths of kaonic atoms [14], as one can see in fig. 2.

A fit to the global set of kaonic atoms data was carried out in [15], where it was concluded that a best fit potential could be achieved with a moderate increase by about 20 % of the theoretical potential of [10].

It is most opportune to mention here that the discrepancies of the theory with experiment for the shift of the ${}^4\text{He}$ data in fig. 2 have been resolved recently, thanks to a technological breakthrough in the work of [16]. It is also interesting to note that this discrepancy has been used in the past to justify that the kaon nucleus potential had to have much larger strength [17,18]. The new experimental findings rule out these superstrong potentials with as much as 600 MeV attraction at the center of the nucleus.

5 Deeply Bound Kaon Atoms

The potential of [10] is sufficiently strong to produce deeply bound kaonic states. It produces indeed a 1s deeply bound state around 30 MeV. It produces also a p state bound by 10 MeV. The problem in both cases is that the states have a width of about 100 MeV. This is much bigger than the

separation between the levels and precludes the experimental observation of peaks. This is the situation of the deeply bound kaon atoms in the context of chiral theories, which have proved to be highly accurate to deal with meson baryon and meson nucleus interaction.

The issue of the kaon interaction in the nucleus has attracted much attention in past years. Although from the study of kaon atoms one knows that the K^- -nucleus potential is attractive [19], the discussion centers on how attractive the potential is and if it can accommodate deeply bound kaon atoms (kaonic nuclei), which could be observed in direct reactions. A sufficiently large attraction could even make possible the existence of kaon condensates in nuclei, which has been suggested in [20]. The list of papers where strongly attractive potentials are used is long [21,22,23,24,25,26,27,28], providing as much as 200 MeV attraction at normal nuclear matter. More moderate attraction is found in similar works done in [29,30,31]. Yet, all modern potentials based on underlying chiral dynamics of the kaon-nucleon interaction [9,10,11,12,13] lead to moderate potentials of the order of 60 MeV attraction at nuclear matter density. They also have a large imaginary part which makes the width of the deeply bound states much larger than the energy separation between the levels, which would rule out the experimental observation of peaks.

The opposite extreme is represented by some highly attractive phenomenological potentials with about 600 MeV strength in the center of the nucleus [17,18]. These potentials, leading to compressed nuclear matter of ten times nuclear matter density, met criticisms from [32] and more recently from [33], which were rebutted in [34] and followed by further argumentation in [35] and [36]. More recently the lightest K-nuclear system of $\bar{K}NN$ has also been the subject of strong debate [37,38,39,40].

Experimentally, the great excitement generated by peaks seen at KEK [41] and FINUDA [42,43], originally interpreted in terms of deeply bound kaons atoms, has calmed down, particularly after the work of [32] regarding the KEK experiment and of [44,45,46] regarding the FINUDA ones found explanations of the experimental peaks based on conventional reactions that unavoidably occur in the process of kaon absorption. Also the thoughts of [47], with opposite views to those of FINUDA in [42], and the reanalysis of the KEK experiment of [41] done in [47], where the original narrow peak appears much broader, have helped to bring the discussion to more realistic terms. In any case, this short discussion has served to show the intense activity and interest in the subject.

There is however one experiment from where the authors claim evidence for a very strong kaon-nucleons potential, of the order of 200 MeV attraction [48]. The experiment looks for fast protons coming out from the absorption of kaons in flight in nuclei. The problem has been recently studied in [49] where it was shown how the experiment was analyzed and which ingredients are missing in the analysis of [48].

One of the shortcomings of [48] stems from the use of the Green's function method [50] in a variant used in [51,52,53] to analyze the data and extract from there the

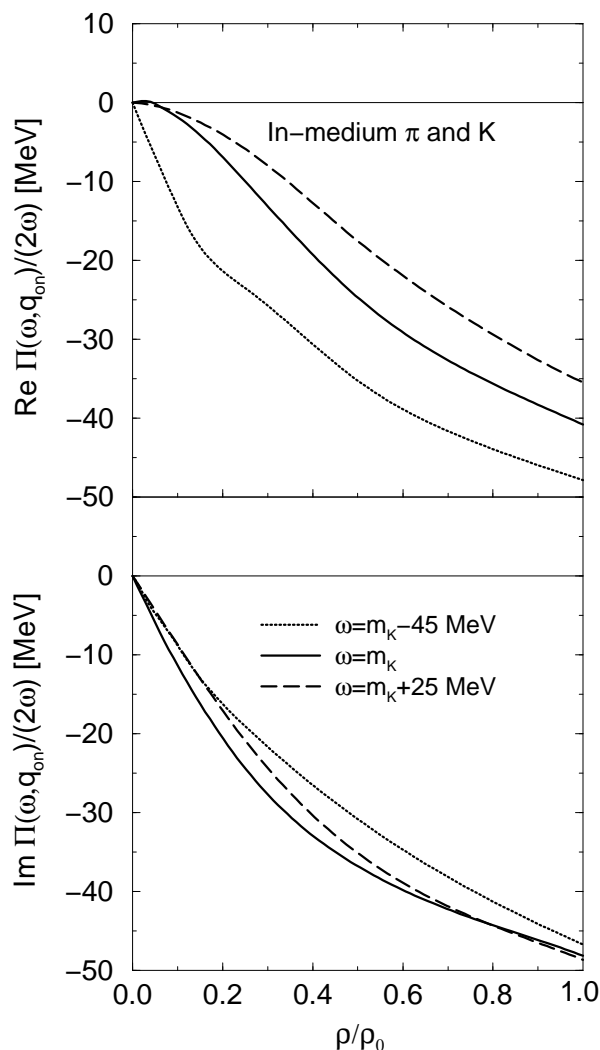


Figure 1. Real (top) and imaginary (bottom) parts of the K^- optical potential as a function of density obtained from the *In-medium pions and kaons* approximation. Results are shown for three different K^- energies: $\omega = m_K - 45$ MeV (dotted lines), $\omega = m_K$ (solid lines) and $\omega = m_K + 20$ MeV (dashed lines).

kaon optical potential. The only mechanism considered in [48] for the emission of fast protons is the $\bar{K}N \rightarrow \bar{K}N$, taking into account the optical potential for the kaon in the final state. However, in [49] one can see that there are other mechanisms that contribute to the emission of fast protons. One of the mechanisms is the kaon absorption by one nucleon, $K^-N \rightarrow \pi\Sigma$ or $K^-N \rightarrow \pi\Lambda$ followed by decay of the Σ or the Λ into πN . Another of the mechanisms is the absorption of kaons by pairs of nucleons, $\bar{K}NN \rightarrow \Sigma N$ and $\bar{K}NN \rightarrow \Lambda N$, followed by similar hyperon decays. The contributions from these processes were also suggested in Ref. [51]. Another important point disclosed in [49] is that in the experiment of [48] there was an extra requirement of coincidence: in addition to a fast proton detected forward one demanded that there would be at least a charged particle detected in a layer counter surrounding the target. It was assumed in [48] that this does not change the shape of the proton distribution, but it was found in [49] that this is not the case and the shape of the spectrum changes substantially, to the point of invalidating the conclusions

drawn in [48]. Although in [49] one does not make claims for a certain strength of the kaon potential, because the reaction is not particularly suited to determine this magnitude, one at least finds that a shallow potential is preferred to a very strong one.

6 Correlated Λd pairs emitted after the absorption of kaons at rest in nuclei

As an example of how one does interpret experiments which have been advocated as evidence for deeply bound kaon atoms in nuclei we explain here the case in favor of a deeply bound kaon from a peak seen in the experiment of [43]. In this experiment Λ and d were measured in coincidence after kaon absorption at rest from ${}^6\text{Li}$ and ${}^{12}\text{C}$, and it was observed that the Λ and d were strongly correlated back to back. From there the authors concluded the formation of a bound state of a kaon and three nucleons which decays in Λd .

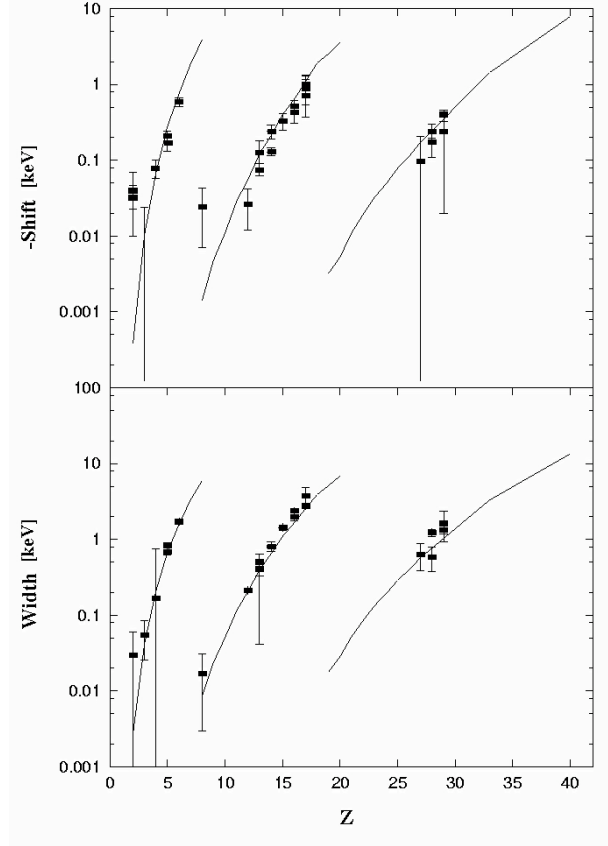


Figure 2. Energy shifts and widths of kaonic atom states (from [14]). . From left to right the states correspond to the 2p,3d and 4f atomic levels.

In the $K_{stop}^- A \rightarrow \Lambda d A'$ reaction [43], at least three nucleons must participate in the absorption process. Two body K^- absorption processes of the type $K^- NN \rightarrow \Sigma N(\Lambda N)$ have been studied experimentally in [54] and their strength is seen to be smaller than that of the one body absorption $K^- N \rightarrow \pi \Sigma(\pi \Lambda)$ mechanisms. This result follows the argument that it is easier to find one nucleon than two nucleons together in the nucleus. This is also the case in pion absorption in nuclei, where extensive studies, both theoretical [55] and experimental [56], obtain the direct two and three body absorption rates with the former one dominating over the later, particularly for pions of low energy. We follow here the same logics and assume the process to be dominated by direct three body K^- absorption, the four body playing a minor role.

The former assumption means in practice that, in ${}^6\text{Li}$, the other three nucleons not directly involved in the absorption process will be spectators in the reaction. These three spectator nucleons have to leave the nucleus, but they were originally bound in the nucleus. The nuclear dynamics takes care of this since there is a distribution of momenta and energies in the nucleus, and the ejection of ei-

ther three nucleons, a nd pair or tritium, implies that the absorption is done in the most bound nucleons.

The other element of relevance is the atomic orbit from which the kaon is absorbed. This information is provided by the last measured transition in the X-ray spectroscopy of K^- -atoms, which occurs precisely because absorption overcomes the γ ray emission. In the case of ${}^6\text{Li}$ this happens for the $2p$ atomic state [14,19].

Following the line of studies done for pion absorption and other inclusive reactions [57], we describe the nucleus in terms of a local Fermi sea with Fermi momentum $k_F(r)$. The nucleons move in a mean field given by the Thomas Fermi potential

$$V(r) = -\frac{k_F^2(r)}{2m_N}, \quad k_F(r) = \left(\frac{3\pi^2}{2}\rho(r)\right)^{1/3}, \quad (14)$$

where m_N is the nucleon mass and $\rho(r)$ is the local nucleon density inside the nucleus.

This potential assumes a continuity from the energies of the bound states (holes) to those in the continuum (particles), which is not the case in real nuclei. For this reason, we implement an energy gap, Δ , which is adjusted to

respect the threshold of the reaction. The introduction of a gap in the Fermi sea is a common practice in order to be precise with the actual binding energies of the nuclei involved in a particular reaction so that the corresponding threshold is respected [58,59,60]. Hence, we demand that the highest possible invariant mass of K^-NNN system, which happens when the three nucleons are at the Fermi surface with total three-momentum zero, corresponds to the minimum possible energy for a spectator three-nucleon system with total zero momentum, namely a tritium at rest. This situation corresponds to

$$m_{K^-} + M_{6\text{Li}} = m_{K^-} + 3m_N - 3\Delta + M_t, \quad (15)$$

and we determine $\Delta = 7.8$ MeV. In the above expression m_{K^-} , M_t , $M_{6\text{Li}}$ are the masses of the corresponding particles and nuclei.

The probability of K^- absorption by three nucleons will be determined from the third power of the nuclear density as

$$\Gamma \propto \int d^3\mathbf{r} |\Psi_{K^-}(r)|^2 \rho^3(r), \quad (16)$$

where $\Psi_{K^-}(r)$ is the K^- atomic wave function. In order to take into account the Fermi motion we write the density as $\rho(r) = 4 \int \frac{d^3\mathbf{p}}{(2\pi)^3} \Theta(k_F(r) - |\mathbf{p}|)$ and then we obtain

$$\Gamma \propto \int d^3\mathbf{r} d^3\mathbf{p}_1 d^3\mathbf{p}_2 d^3\mathbf{p}_3 |\Psi_{K^-}(r)|^2 \times \Theta(k_F(r) - |\mathbf{p}_1|) \Theta(k_F(r) - |\mathbf{p}_2|) \Theta(k_F(r) - |\mathbf{p}_3|). \quad (17)$$

From this expression we can evaluate all observables of the reaction. Let us first concentrate on the Λd invariant mass which, for each $K^-NNN \rightarrow \Lambda d$ decay event, is precisely the invariant mass of the corresponding K^-NNN system, the other three nucleons acting as spectators. Thus the energy of the Λd pair is obtained from

$$E_{\Lambda d} = E_{K^-NNN} \equiv E_{K^-} + E_{N_1} + E_{N_2} + E_{N_3} \quad (18)$$

$$= m_{K^-} + 3m_N + \frac{\mathbf{p}_1^2}{2m_N} + \frac{\mathbf{p}_2^2}{2m_N} + \frac{\mathbf{p}_3^2}{2m_N} - 3 \frac{k_F^2(r)}{2m_N} - 3\Delta,$$

and the momentum from

$$\mathbf{P}_{\Lambda d} = \mathbf{P}_{K^-NNN} = \mathbf{p}_1 + \mathbf{p}_2 + \mathbf{p}_3, \quad (19)$$

and, correspondingly,

$$M_{\Lambda d} = E_{\Lambda d} - \frac{\mathbf{P}_{\Lambda d}^2}{2E_{\Lambda d}}. \quad (20)$$

One may also easily obtain the invariant mass of the residual system, M^* , from

$$M^* = E^* - \frac{\mathbf{P}^{*2}}{2E^*}, \quad (21)$$

with

$$E^* = m_{K^-} + M_{6\text{Li}} - E_{K^-NNN}, \quad \mathbf{P}^* = -\mathbf{P}_{\Lambda d}. \quad (22)$$

Each event in the multiple integral of Eq. (17), done with the Monte Carlo method, selects particular values for \mathbf{r} , \mathbf{p}_1 , \mathbf{p}_2 and \mathbf{p}_3 which, in turn, determine the value of the corresponding Λd invariant mass from Eqs. (19)–(20). Since the minimum obvious invariant mass of the residual three-nucleon system is $M^* = M_t$, corresponding to the emission of tritium, the cut $\Theta(M^* - M_t)$ is also imposed for each event. A compilation of events provides us with the Λd invariant mass distribution. We also directly obtain the distribution of total Λd momentum, Eq. (19), to be directly compared with the Λd momentum measured in [43].

Note that the model presented here is a straightforward generalization (from two nucleon to three nucleon K^- absorption) of the one used in Refs. [44,61], however here we concentrate on the primary reaction peak, while in Refs. [44,61] the authors were more interested in the peak generated by the final state interactions, i.e. by the collisions of the primary produced Λ and p on their way out of the nucleus. Since the two nucleon K^- absorption, discussed in [44,61], was measured for heavier nuclei [42], the final state interaction peak was stronger than that of the primary reaction, contrary to the reaction studied in this work.

Other observables measured in [43] require an additional work. One is the angular correlation of Λd pairs, and the other is the missing mass assuming a residual nd system, apart from the measured Λd pair, namely

$$T_{\text{miss}} = m_{K^-} + M_{6\text{Li}} - m_{\Lambda} - m_n - 2M_d - (T_{\Lambda} + T_d), \quad (23)$$

where m_{Λ} , M_d and T_{Λ} , T_d are the masses and the kinetic energies of the Λ and the d , correspondingly. These two observables require the evaluation of the individual Λ and d momenta in the laboratory frame. Their value in the center of mass (CM) frame of the Λd pair is given in terms of the known invariant mass but their direction in this frame is arbitrary. We take this into account by obtaining Λ and d momenta in the CM frame

$$\mathbf{p}_{\Lambda}^{\text{CM}} = p_{\Lambda}^{\text{CM}} (\sin \Theta \cos \phi, \sin \Theta \sin \phi, \cos \Theta), \quad (24)$$

$$\mathbf{p}_d^{\text{CM}} = -\mathbf{p}_{\Lambda}^{\text{CM}},$$

with

$$p_{\Lambda}^{\text{CM}} = \frac{\lambda^{1/2}(M_{\Lambda d}^2, m_{\Lambda}^2, M_d^2)}{2M_{\Lambda d}}, \quad (25)$$

where the events are now generated according to the distribution provided by the integral

$$\int d \cos \Theta \int d \phi \int d^3\mathbf{r} d^3\mathbf{p}_1 d^3\mathbf{p}_2 d^3\mathbf{p}_3 |\Psi_{K^-}(r)|^2 \times \Theta(k_F(r) - |\mathbf{p}_1|) \Theta(k_F(r) - |\mathbf{p}_2|) \Theta(k_F(r) - |\mathbf{p}_3|) \times \Theta(M^* - M_t). \quad (26)$$

In order to have the final Λ and d momenta in the laboratory frame, where the Λd pair has momentum $\mathbf{P}_{\Lambda d}$, we apply the transformations

$$\mathbf{p}_{\Lambda} = \mathbf{p}_{\Lambda}^{\text{CM}} + m_{\Lambda} \mathbf{v}$$

$$\mathbf{p}_d = -\mathbf{p}_{\Lambda}^{\text{CM}} + M_d \mathbf{v}, \quad (27)$$

where $\mathbf{v} = \mathbf{P}_{\Lambda d} / (m_{\Lambda} + M_d)$. These last equations allow us to find the cosine of the angle between the directions of Λ

and d . Therefore, generating the distribution of events according to their relative angle is straightforward. We see, as it is also the case of the experiment, that $P_{\Lambda d} \sim 200$ MeV/c, while $p_{\Lambda}^{CM} \sim 650$ MeV/c, which already guarantees that the Λd events are largely correlated back-to-back.

We note that our calculations incorporate the same momentum cuts as in the experiment, namely $140 \text{ MeV/c} < p_{\Lambda} < 700 \text{ MeV/c}$ and $300 \text{ MeV/c} < p_d < 800 \text{ MeV/c}$.

In Fig. 3 we show the results for the invariant mass of the Λd system. Our distribution, displayed with a dot-dashed line, peaks around $M_{\Lambda d} = 3252$ MeV as in the experiment. The shape of the distribution also compares remarkably well with the experimental histogram in the region of the peak, which is the energy range that we are exploring in the present work. We obtain a width of about 36 MeV, as reported in the experiment. Note that apart from the peak that we are discussing, the experiment also finds events at lower Λd invariant masses which did not play a role in their discussion [43]. These events would be generated in cases where there is final state interaction of the Λ or the d with the rest of the nucleons, as was discussed in [44,61], or through other absorption mechanisms.

The angular correlations between the emitted Λ and d can be seen in the distribution displayed in Fig. 4, where, as in the experimental analysis, we consider only those events which fall in the region $3220 \text{ MeV} < M_{\Lambda d} < 3280 \text{ MeV}$. As we can see in the figure, the distribution is strongly peaked backward and the agreement with experiment is very good.

One also finds good agreement with data for the distribution of the total Λd momentum and the missing mass distribution.

7 The $\bar{K}NN$ system

In the context of low-energy QCD with $N_f = 3$ quark flavors, the study of possible antikaon-nuclear quasibound states is a topic of great current interest. Spontaneously broken chiral $SU(3) \times SU(3)$ symmetry, together with explicit symmetry breaking by the non-zero quark masses, basically determines the leading couplings between the low-mass pseudoscalar meson octet (Nambu-Goldstone bosons in the chiral limit) and the octet of the ground state baryons. In particular, the Tomozawa-Weinberg chiral low-energy theorem implies that the driving $\bar{K}N$ interaction in the isospin $I = 0$ channel is strongly attractive. Likewise, the $I = 0$ $\pi\Sigma$ interaction is attractive. The coupling between these $\bar{K}N$ and $\pi\Sigma$ channels is the prime feature governing the sub-threshold extrapolation of the $\bar{K}N$ interaction.

We have already discussed the problem of the K^- -nucleus interaction and K^- bound states. A prototype system for these considerations is ppK^- , the simplest antikaon-nuclear cluster. It has recently been investigated using three-body methods with Faddeev equations [37,39] and variational approaches [40,62,63,?]. Reaction studies [64] have also been performed dealing with the actual formation of ppK^- . The Faddeev and variational calculations predict a total ppK^- binding energy in a range $B \sim 50 - 70$ MeV, together with an estimate of the $\bar{K}NN \rightarrow \pi YN$ decay width,

$\Gamma \sim 50 - 100$ MeV, depending on details of the interactions used.

The key issue in any such calculation is the extrapolation of the $\bar{K}N$ interaction into the region far below threshold. Its predictive power is limited by the lack of accurate constraints from data.

Apart from the constraints provided by $\bar{K}N$ threshold data and low-energy cross sections, the only piece of information about the interaction below $\bar{K}N$ threshold is the $\pi\Sigma$ mass spectrum which is dominated by the $\Lambda(1405)$ resonance. In [38] the extrapolation below threshold of the effective $\bar{K}N$ interaction has been done following [33] from the viewpoint of chiral $SU(3)$ dynamics. Their structure shares features with the pioneering coupled-channel model [65] that used vector meson exchange interactions (see also Ref. [66]).

Most chiral $SU(3)$ based calculations produce two $\Lambda(1405)$ states which are seen in the $\pi\Sigma$ mass spectrum [67]. The higher mass state peaks around 1420 MeV and is relatively narrow, while the lower mass state is more uncertain but peaks around 1395 MeV and is much wider. This implies that the effective single-channel $\bar{K}N$ interaction is substantially weaker than anticipated in the simple phenomenological potential of [17,18]. In those phenomenological studies, the local, energy-independent potential was adjusted interpreting the $\Lambda(1405)$ directly as a $\bar{K}N$ bound state, identifying its binding energy by the location of the maximum observed in the $\pi\Sigma$ spectrum of the reaction of [68], but ignoring strong coupled-channel effects.

In [38] a variational ppK^- calculation was performed employing the new effective $\bar{K}N$ potential derived from chiral coupled-channel dynamics in [33], together with a realistic NN potential. This calculation is supposed to be complementary to the Faddeev approach with chiral $SU(3)$ constraints [39]. The variational calculation gives easy access to the wave function of the bound state so that valuable information about the structure of the ppK^- cluster can be extracted, whereas the elimination of the $\pi\Sigma$ channel is required and the width of the state can only be estimated perturbatively. The Faddeev calculation has, in turn, the advantage that the decay width of the quasibound state is computed consistently in the coupled-channel framework. Both methods therefore have their virtues and limitations.

The work of [38] extends and improves the previous studies [62] in several directions, including further refinements in the NN interaction, computation of density distributions, an evaluation of effects from p -wave $\bar{K}N$ interactions and an estimate of the $\bar{K}NN \rightarrow YN$ absorptive width.

The present situation is rather uncertain and the values of the bindings vary from about 20 to 70 MeV and the width from about 50 to 100 MeV. The different way in which the two body amplitudes are extrapolated off shell might be partly responsible in these three body calculations for the differences in those approaches. In this sense, in section 9.1 we shall present a method to deal with Faddeev equations in coupled channels which eliminates from the beginning this unphysical part of the scattering amplitudes.

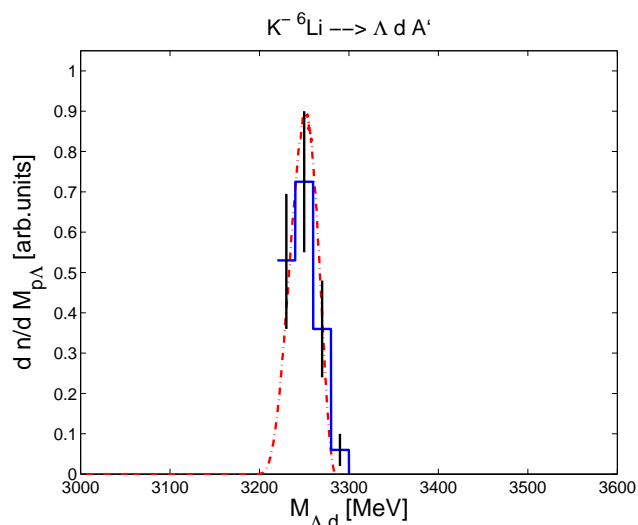


Figure 3. (Color online) The Λd invariant mass distribution for the $K_{stop}^- A \rightarrow \Lambda d A'$ reaction. Histogram and error bars are from the experimental paper [43], while the dot-dashed curve is the result of our calculation.

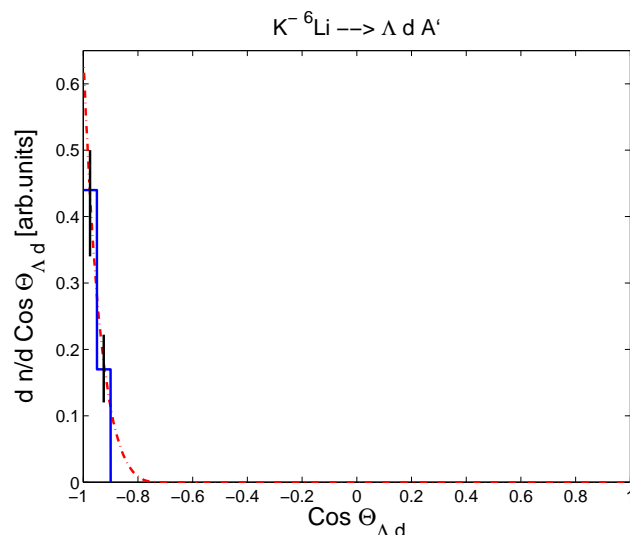


Figure 4. (Color online) The Λd angular distribution for the $K_{stop}^- A \rightarrow \Lambda d A'$ reaction. Histogram and error bars are from the experiment [43], while the dot-dashed curve is the result of our calculation. As in the experimental analysis, we take into account the following cuts: $3220 \text{ MeV} < M_{\Lambda d} < 3280 \text{ MeV}$.

8 Conclusion on experimental situation on deeply bound kaon clusters

No evidence of deeply bound K^- states on nuclei has been found. All peaks claimed as states could be interpreted in terms of conventional, unavoidable and controllable reactions. Work continues searching for these states in JPARC, FINUDA, AMADEUS, DISTO (see talks by Shevchenko, Morton, Grishina, Vazquez Poce, Lio, Okada Camerini and Tsukada in this Conference). On the positive side, we are learning new and interesting physics about \bar{K} absorption by two and three nucleons, which is relevant from the many body point of view.

9 Other kaonic clusters

In this section I want to call the attention to new and very interesting kaonic clusters which have been investigated only in the last couple of years. I will mention the system with two meson and a baryon, with one of the mesons being a kaon. Some of these three body systems are bound, or form resonances, and lead to the low lying $1/2^+$ excited baryons with strangeness. The other systems are also three body systems with a cluster of $K\bar{K}$, one of them with an extra nucleon, another one with an extra ϕ meson and the third one with a J/ψ . The study of these new systems has been stimulated by a reformulation of the Faddeev equations within the formalism of the chiral unitary approach [69,70].

9.1 Formalism

We solve Faddeev equations in the coupled channel approach. These coupled systems have first been constructed by pairing up all the possible pseudoscalar mesons and $1/2^+$ baryons, which couple to strangeness $=-1$, and adding a pion to the pair finally. One ends up with twenty-two coupled channels for a fixed total charge [69]. The interaction in the meson-baryon sub-systems has been written in S -wave, which implies, after adding another meson in S -wave, that the total J^P of the three body system is $1/2^+$.

The solution of the Faddeev equations,

$$T = T^1 + T^2 + T^3, \quad (28)$$

where the T^i partitions are written in terms of two body t -matrices (t^i) and three body propagators ($g = [E - H]^{-1}$) as

$$T^i = t^i + t^j g [T^j + T^k] \quad (i \neq j, i, j \neq k = 1, 2, 3), \quad (29)$$

requires off-shell two body t -matrices as an input. However, we found that the off-shell contributions of the two body t -matrices give rise to three-body forces which, when summed up for different diagrams, cancel the one arising directly from the chiral Lagrangian in the $SU(3)$ limit [69]. In the realistic case, this sum was found to be only 5 % of the total on-shell contribution [69]. Thus, it is reasonably accurate to study the problem by solving the Faddeev equations with the on-shell two-body t -matrices and by neglecting the three-body forces.

In this way, a term at second order in t in the Faddeev partitions (fig. 5), for instance,

$$t^1 g^{13} t^3, \quad (30)$$

is written as a product of the on-shell two body t -matrices t^1 and t^3 and the propagator g^{13} given as

$$g^{13} = \frac{1}{2E_2} \frac{1}{\sqrt{s} - E_1(\mathbf{k}'_1) - E_2(\mathbf{k}'_1 + \mathbf{k}_3) - E_3(\mathbf{k}_3) + i\epsilon}.$$

Adding another interaction to the diagram in fig. 5 (see fig. 6), the expression $t^1 g^{13} t^3$ gets extended to $t^2 g^{21} t^1 g^{13} t^3$, which can be written explicitly as

$$\begin{aligned} & t^2(s_{13}) \left[\int \frac{d\mathbf{k}''}{(2\pi)^3} \frac{1}{2E_1(\mathbf{k}'') + \mathbf{k}_3} \frac{1}{2E_2(\mathbf{k}'' + \mathbf{k}_3)} \frac{2M_3}{2E_3(\mathbf{k}'' + \mathbf{k}'_2)} \right. \\ & \times \frac{t^1(s_{23}(\mathbf{k}''))}{\sqrt{s} - E_1(\mathbf{k}'') - E_2(\mathbf{k}'_2) - E_3(\mathbf{k}'' + \mathbf{k}'_2) + i\epsilon} \\ & \left. \times \frac{1}{\sqrt{s} - E_1(\mathbf{k}'') - E_2(\mathbf{k}'' + \mathbf{k}_3) - E_3(\mathbf{k}_3) + i\epsilon} \right] t^3(s_{12}), \end{aligned}$$

where $s_{13} = (P - K_2)^2$, $s_{12} = (P - K_3)^2$, $s_{23}(\mathbf{k}'') = (P - K'')^2$ with P, K_3, K'_2 and K'' representing the four momenta corresponding to the $\mathbf{P} = 0, \mathbf{k}_3, \mathbf{k}'_2$ and \mathbf{k}'' respectively. Our aim is to extract $t^1 g^{13} t^3$ out of the integral, which could simplify the calculations. The $t^2(s_{13})$ and $t^3(s_{12})$, in the

equation above, depend on on-shell variables and can be factorized out of the loop integral but not t^1 and g^{13} [69]. This can be done if we re-arrange the loop integral as is done in [69].

There one defines a function F^{ijk} which includes the loop variable dependence of t^j . Then one defines a function G^{ijk} as

$$G^{213} = \int \frac{d\mathbf{k}''}{(2\pi)^3} \frac{1}{2E_1(\mathbf{k}'')} \frac{2M_3}{2E_3(\mathbf{k}'')} \frac{F^{213}(\sqrt{s}, \mathbf{k}'')}{\sqrt{s_{13}} - E_1(\mathbf{k}'') - E_3(\mathbf{k}'') + i\epsilon}$$

The diagram in fig. 6 can, hence, be re-written as $t^2 G^{213} t^1 g^{13} t^3$. The formalism has been developed following the above procedure, i.e., by replacing g by G , every time a new interaction is added. This leads to another form of the Faddeev partitions (eq. (29)), which, after removing the terms corresponding to the disconnected diagrams and by denoting the rest of the equation as T_R , can be re-written as

$$T_R^{ij} = t^i g^{ij} t^j + t^i G^{ijk} T_R^{jk} + t^i G^{iji} T_R^{ji}, \quad i \neq j, j \neq k = 1, 2, 3. \quad (31)$$

The T_R^{ij} can be related to the Faddeev partitions (eq. (29)) as $T^i = t^i + T_R^{ij} + T_R^{ik}$, hence, giving six coupled equations instead of three (eq. (29)). These T_R^{ij} partitions correspond to the sum of all the possible diagrams with the last two interactions written in terms of t^i and t^j . This regrouping of diagrams is done for the sake of convenience due to the different forms of the G^{ijk} functions. We define T_R as

$$T_R = \sum_{i \neq j=1}^3 T_R^{ij}, \quad (32)$$

which can be related to the sum of the Faddeev partitions (eq. (28)) as

$$T = t^1 + t^2 + t^3 + T_R. \quad (33)$$

9.2 Results and discussion

One constructs the three-body T_R -matrices using the isospin symmetry, for which we must take an average mass for the isospin multiplets π (π^+, π^0, π^-), \bar{K} (\bar{K}^0, K^-), K (K^+, K^0), N (p, n), Σ ($\Sigma^+, \Sigma^0, \Sigma^-$) and Ξ (Ξ^0, Ξ^-). In order to identify the nature of the resulting states, we project the T_R -matrix on the isospin base. One appropriate base is the one where the states are classified by the total isospin of the three particles, I , and the total isospin of the two mesons, I_π in the case of two pions. Using the phase convention $|\pi^+\rangle = -|1, 1\rangle$, $|K^-\rangle = -|1/2, -1/2\rangle$, $|\Sigma^+\rangle = -|1, 1\rangle$ and $|\Xi^-\rangle = -|1/2, -1/2\rangle$ we have, for example, for the $\pi\pi\Sigma$ channel

$$\begin{aligned} |\pi^0 \pi^0 \Sigma^0\rangle &= |1, 0\rangle_\pi \otimes |1, 0\rangle_\pi \otimes |1, 0\rangle_\Sigma \\ &= \left\{ \sqrt{\frac{2}{3}} |2, 0\rangle - \sqrt{\frac{1}{3}} |0, 0\rangle \right\}_{\pi\pi} \otimes |1, 0\rangle_\Sigma \\ &= \sqrt{\frac{2}{5}} |I = 3, I_\pi = 2\rangle - \frac{2}{\sqrt{15}} |I = 1, I_\pi = 2\rangle - \end{aligned}$$

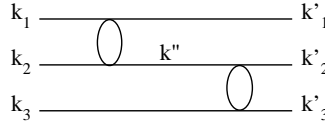


Figure 5. The diagrammatic representation of the $t^1 g t^3$ term.

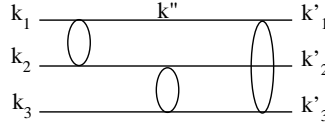


Figure 6. The diagrammatic representation of $t^2 g^{21} t^1 g^{13} t^3$.

$$-\sqrt{\frac{1}{3}} |I = 1, I_\pi = 0\rangle,$$

where, I and I_π denote the total isospin of the three body system and that of the two pion system, respectively. Similarly, we write the other states in the isospin base.

After projecting the T_R -matrix (eq. (32)) on the isospin base, we square them and plot them as a function of the total energy (\sqrt{s}) of the two meson one baryon system and the invariant mass of particles 2 and 3 ($\sqrt{s_{23}}$). However, this choice is arbitrary, we could as well plot the squared amplitude, for example, as a function of $\sqrt{s_{12}}$ and $\sqrt{s_{13}}$.

In fig. 7, we show our results for $\pi\pi\Lambda$ in the $|I, I_\pi\rangle = |0, 0\rangle$ case, where a peak at 1740 MeV is clearly seen. The full width at half maximum of this peak is ~ 20 MeV. We identify this resonant structure with the $\Lambda(1810)$ in the particle data book [71]. It should be noted that, even though the status of this resonance in [71] is three-star, the associated pole positions vary from about 1750 MeV to 1850 MeV and the corresponding widths from 50-250 MeV.

We find evidence for two more resonances in the isospin zero sector in the $\Lambda(1600)$ region. Apart from this, we find evidence for four low-lying Σ resonances: 1) for the $\Sigma(1560)$, thus predicting $J^P = 1/2^+$ for it, 2) the $\Sigma(1620)$, for which the partial-wave analyses and experimental findings are kept separately in the *PDG*, 3) the well-established $\Sigma(1660)$ and 4) the one-star $\Sigma(1770)$. All these results are summarized in the table 1, along with the states listed by the Particle Data Group.

9.3 The $\bar{K}\pi N$ and coupled channels system

In [69] a total of 22 coupled channels to $\bar{K}\pi N$ were considered. The T matrix was projected over total isospin states and the $|T|^2$ matrix was plotted against two variables, the total energy and the invariant mass of a pair of particles, either a meson and a baryon of the two mesons. The magnitude $|T|^2$ exhibits clear peaks around a value of $\sqrt{s_{23}}$ and \sqrt{s} . This tell us not only that there is a resonance at a certain energy but also that the pair of particles considered are highly correlated around th energy at the peak. Usually this corresponds to the energy where the pair considered forms a dynamically generated resonance from meson baryon like the $\Lambda(1405)$ or from two mesons ($K\bar{K}$ and $\pi\pi$) like the $f_0(980)$. In table 1 we show the summary of the results obtained

Table 1. A comparison of the resonances found in this work with the states in *PDG*.

	Γ (<i>PDG</i>) (MeV)	Peak position (this work, MeV)	Γ (this work) (MeV)
Isospin = 1			
$\Sigma(1560)$	10 - 100	1590	70
$\Sigma(1620)$	10 - 100	1630	39
$\Sigma(1660)$	40 - 200	1656	30
$\Sigma(1770)$	60 - 100	1790	24
Isospin = 0			
$\Lambda(1600)$	50 - 250	1568,1700	60,135
$\Lambda(1810)$	50 - 250	1740	20

9.4 State of $K\bar{K}N$ and coupled channels

In [72] using a variational method and chiral dynamics for the interaction of the kaons with nucleons a bound state of the $K\bar{K}N$ system was found, where the $K\bar{K}$ system was forming the $a_0(980)$ resonance. The importance of using coupled channels has been made patent in [69,70]. In this sense the idea of [72] was retaken in [73] using coupled channels. The paper also had a novel idea. The fact that it was found that there was a cancellation between the off shell part of the two body amplitudes and the three body amplitudes coming from the same chiral Lagrangians was understood as some thing more profound, that in this problems one can use on shell amplitudes and not worry about three body forces, and of course the on shell two body amplitudes can be obtained from experiment and used beyond the region of applicability of the chiral unitary approach that relies only on the lowest order chiral Lagrangian and absence of possible genuine resonances (or dynamically generated from other components than those taken into account). In this sense, in [73] this idea was put to work taking experimental amplitudes for πN above 1600 MeV, where the chiral theory [74] fails to deal with the $N^*(1650)$ resonance.

Many baryon resonances are found in [73] with strangeness zero, but we are only interested here on the state made out from $K\bar{K}N$ and coupled channels. We find that in spite of the adding new channels into the approach, the results of

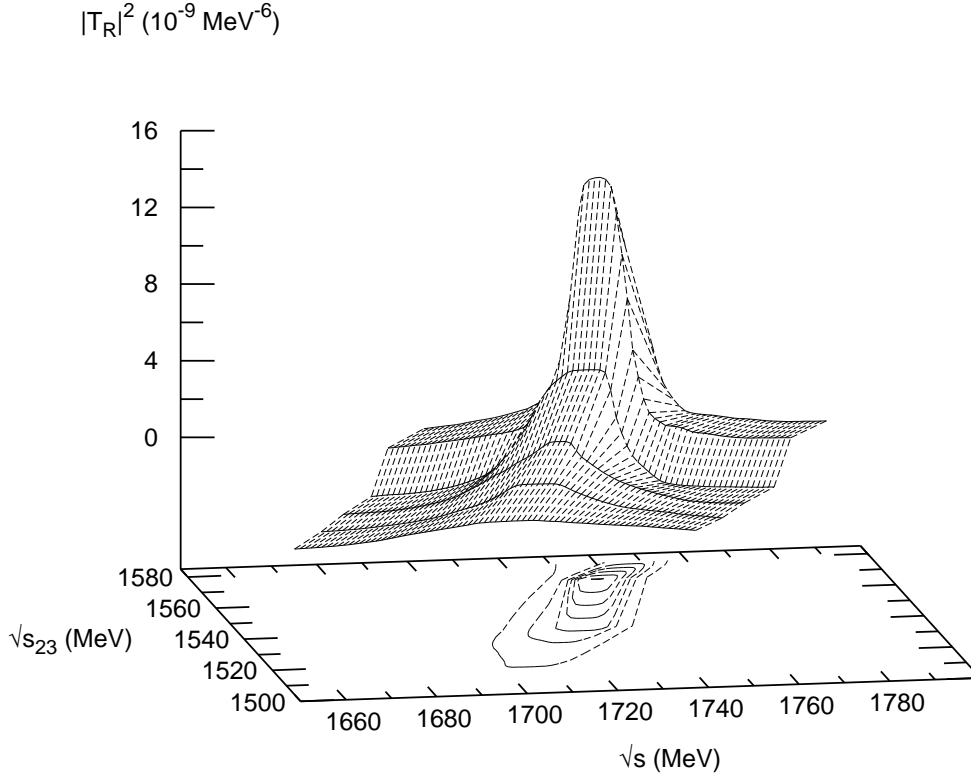


Figure 7. The $\Lambda(1810)$ resonance depicted in the squared amplitude for $\pi\pi\Lambda$ in the $|I, I_\pi\rangle = |0, 0\rangle$ configuration.

[72] remain and a resonance appears around the energy predicted in [72]. There is only a small novelty, the $K\bar{K}$ clusters in our approach both around the $f_0(980)$ and the $a_0(980)$, while in [72] it was mostly a $a_0(980)N$ state.

It is interesting to note that such a state around 1920 MeV, could have already been seen. This is the idea behind the work of [75] which claims that this state could correspond to the peak seen in the $\gamma p \rightarrow K^+\Lambda$ reaction as we discuss in the next subsection.

9.5 Comparison of the $\gamma p \rightarrow K^+\Lambda$ and $\gamma p \rightarrow K^+\Sigma^0$ reactions

A peak of moderate strength on top of a large background is clearly seen for the $\gamma p \rightarrow K^+\Lambda$ reaction around 1920 MeV at all angles (see Fig. 18 of [76]). One can induce qualitatively a width for this peak of about 100 MeV or less. On the other hand, if one looks at the $\gamma p \rightarrow K^+\Sigma^0$ reaction, one finds that starting from threshold a big large and broad structure develops, also visible at all angles (see Fig. 19 of [76]). The width of this structure is about 200-300 MeV. One can argue qualitatively that the relatively narrow peak of the $\gamma p \rightarrow K^+\Lambda$ reaction around 1920 MeV on top of a large background has nothing to do with the broad structure of $\gamma p \rightarrow K^+\Sigma^0$ around 1900 MeV. A more quantitative argument can be provided by recalling that in [77]

the broad structure of the $\gamma p \rightarrow K^+\Sigma^0$ is associated to two broad Λ resonances in their model, which obviously can not produce any peak in the $\gamma p \rightarrow K^+\Lambda$ reaction, which filters isospin 1/2 in the final state. Certainly, part of the structure is background, which is already obtained in chiral unitary theories at the low energies of the reaction [78].

We thus adopt the position that the peak in the $\gamma p \rightarrow K^+\Lambda$ reaction is a genuine isospin 1/2 contribution which does not show up in the $\gamma p \rightarrow K^+\Sigma^0$ reaction. This feature would find a natural interpretation in the picture of the state proposed in [72,73]. Indeed, in those works the state at 1920 MeV is a $K\bar{K}N$ system in relative s-waves for all pairs. The $\gamma p \rightarrow K^+\Lambda$ and $\gamma p \rightarrow K^+\Sigma^0$ reactions proceeding through the excitation of this resonance are depicted in Fig. 8. The two reactions are identical in this picture, the only difference being the Yukawa coupling of the K^- to the proton to generate either a Λ or a Σ^0 .

The Yukawa couplings in SU(3) are well known and given in terms of the F and D coefficients [79], with $D+F = 1.26$ and $D - F = 0.33$ [80,78]. The particular couplings for $K^-p \rightarrow \Lambda$ and $K^-p \rightarrow \Sigma^0$ are e.g. given in [81].

$$V_{K^-p \rightarrow \Lambda} = -\frac{2}{\sqrt{3}} \frac{D+F}{2f} + \frac{1}{\sqrt{3}} \frac{D-F}{2f} \quad (34)$$

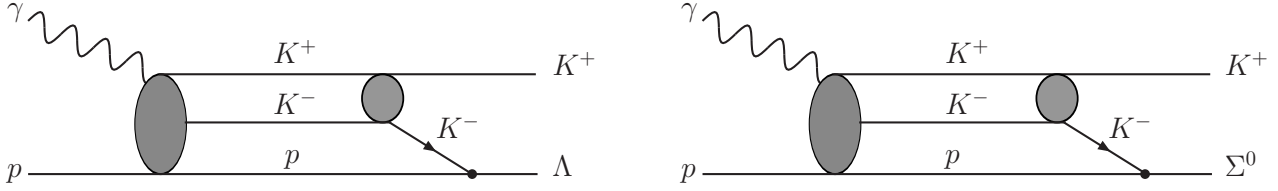


Figure 8. Diagrams depicting the $\gamma p \rightarrow K^+ \Lambda$, $\gamma p \rightarrow K^+ \Sigma^0$ processes through the $1/2^+ N^* K^+ K^- N$ resonance of [73,72].

$$V_{K^- p \rightarrow \Sigma^0} = \frac{D - F}{2f}$$

with f the pion decay constant. Hence, the couplings are proportional to -1.26 and 0.33 for the $K^- p \rightarrow \Lambda$ and $K^- p \rightarrow \Sigma^0$ vertices, respectively. Therefore, it is clear that in this picture the signal of the resonance in the $\gamma p \rightarrow K^+ \Lambda$ reaction is far larger than in the $\gamma p \rightarrow K^+ \Sigma^0$ one, by as much as an order of magnitude in the case that the resonance and background contributions sum incoherently. The $3/2^+$ resonance used in the analysis of the $\gamma p \rightarrow K^+ \Lambda$ reaction in [82] is also used for the $\gamma p \rightarrow K^+ \Sigma^0$ reaction in that work and also give a smaller contribution in this latter case. In the picture of [72,73] the $1/2^+$ resonance also appears in the $\gamma p \rightarrow K^+ \Sigma^0$ reaction but with a smaller intensity than in the $\gamma p \rightarrow K^+ \Lambda$ one, as we have mentioned.

9.6 Test with polarization experiments

In case the $J^P = 1/2^+$ assignment was correct, an easy test can be carried out to rule out the $3/2^+$ state. The experiment consists in performing the $\gamma p \rightarrow K^+ \Lambda$ reaction with a circularly polarized photon with helicity 1, thus $S_z = 1$ with the z -axis defined along the photon direction, together with a polarized proton of the target with $S_z = 1/2$ along the same direction. With this set up, the total spin has $S_z^{tot} = 3/2$. Since L_z is zero with that choice of the z direction, then $J_z^{tot} = 3/2$ and J must be equal or bigger than $3/2$. Should the resonant state be $J^P = 1/2^+$, the peak signal would disappear for this polarization selection, while it would remain if the resonance was a $J^P = 3/2^+$ state. Thus, the disappearance of the signal with this polarization set up would rule out the $J^P = 3/2^+$ assignment.

Such type of polarization set ups have been done and are common in facilities like ELSA at Bonn, MAMI B at Mainz or CEBAF at Jefferson Lab, where spin-3/2 and 1/2 cross sections, which play a crucial role in the GDH sum rule, see e.g. Ref. [83], were measured in the two-pion photoproduction [84,85] reaction. The theoretical analysis of [86] shows indeed that the separation of the amplitudes in the spin channels provides information on the resonances excited in the reaction.

Another test that can be carried out is by looking at the threshold behavior of the cross section for the $\gamma p \rightarrow p K^+ K^-$ reaction. As a consequence of the existence of an s -wave resonance below threshold one finds an enhancement of the cross section around threshold for this reaction, as well as an enhancement of the invariant mass of $K^+ K^-$ close to the sum of the masses of the two kaons, which results from the strong coupling of these two particles to the

$f_0(980)$ and $a_0(980)$ resonances. An experiment on this reaction is already under way and preliminary results already exist at LEPS [87].

10 X(2175) as a resonant state of the $\phi K \bar{K}$ system

The discovery of the X(2175) 1^{--} resonance in $e^+ e^- \rightarrow \phi f_0(980)$ with initial state radiation at BABAR [88,89], also confirmed at BES in $J/\psi \rightarrow \eta \phi f_0(980)$ [90], has stimulated research around its nontrivial nature in terms of quark components. The possibility of it being a tetraquark $s\bar{s}s\bar{s}$ is investigated within QCD sum rules in [91], and as a gluon hybrid $s\bar{s}g$ state has been discussed in [92,93]. A recent review on this issue can be seen in [94], where the basic problem of the expected large decay widths into two mesons of the states of these models, contrary to what is experimentally observed, is discussed. The basic data on this resonance from [88,89] are $M_X = 2175 \pm 10$ MeV and $\Gamma = 58 \pm 16 \pm 20$ MeV, which are consistent with the numbers quoted from BES $M_X = 2186 \pm 10 \pm 6$ MeV and $\Gamma = 65 \pm 25 \pm 17$ MeV. In Ref. [89] an indication of this resonance is seen as an increase of the $K^+ K^- K^+ K^-$ cross section around 2150 MeV. A detailed theoretical study of the $e^+ e^- \rightarrow \phi f_0(980)$ reaction was done in Ref. [95] by means of loop diagrams involving kaons and K^* , using chiral amplitudes for the $K \bar{K} \rightarrow \pi \pi$ channel which contains the $f_0(980)$ pole generated dynamically by the theory. The study revealed that the loop mechanisms reproduced the background but failed to produce the peak around 2175 MeV, thus reinforcing the claims for a new resonance around this mass.

In [96] a very different picture for the X(2175) resonance was advocated which allows for a reliable calculation and leads naturally to a very narrow width and no coupling to two pseudoscalar mesons. The picture is that the X(2175) is an ordinary resonant state of $\phi f_0(980)$ due to the interaction of these components. The $f_0(980)$ resonance is dynamically generated from the interaction of $\pi \pi$ and $K \bar{K}$ treated as coupled channels within the chiral unitary approach of [4,97,98], qualifying as a kind of molecule with $\pi \pi$ and $K \bar{K}$ as its components, with a large coupling to $K \bar{K}$ and a weaker one to $\pi \pi$ [hence, the small width compared to that of the $\sigma(600)$]. Similar studies for the vector-pseudoscalar interaction have also been carried out using chiral dynamics in [99,100], which lead to the dynamical generation of the low-lying axial vectors. In [96] the approach of Ref. [100] to deal with this part of the prob-

lem was used and the ϕK and $\phi\pi$ amplitudes were obtained in that approach.

To study the $\phi f_0(980)$ interaction, one is thus forced to investigate the three-body system $\phi K\bar{K}$ considering the interaction of the three components among themselves and keeping in mind the expected strong correlations of the $K\bar{K}$ system to make the $f_0(980)$ resonance. For this purpose one solves the Faddeev equations with coupled channels $\phi K^+ K^-$ and $\phi K^0 \bar{K}^0$. The picture is later complemented with the addition of the $\phi\pi\pi$ state as a coupled channel. The study benefits from previous ones on the $\pi\bar{K}N$ and $\pi\pi N$ along with their coupled channels done in [101,102], where many $1/2^+$, strange, and nonstrange low-lying baryon resonances of the Particle Data Group [71] were reproduced. This success encouraged us to extend the model of Refs. [101,102] to study the three-meson system, i.e., $\phi K\bar{K}$.

In fig. 9 we show $|T|^2$ as a function of the total energy and the invariant mass of $K\bar{K}$. We find a clear peak around 2150 MeV for the total energy and 980 MeV for the invariant mass of $K\bar{K}$, indicating that we have a resonance made basically from $\phi f_0(980)$, which provides a natural explanation to the experimental features observed for this resonance.

11 The $Y(4260)$ as a $J/\psi K\bar{K}$ system

An enhancement in the data for the $\pi^+\pi^- J/\psi$ invariant mass spectrum was found near 4.26 GeV by the BABAR collaboration in a study of the $e^+e^- \rightarrow \gamma_{ISR}\pi^+\pi^- J/\psi$ process [103]. A fit to this data set was made by assuming a resonance with 4.26 GeV of mass and 50 to 90 MeV of width [103]. The resonance was named as the $Y(4260)$ and it was found to be of $J^{PC} = 1^{--}$ nature. Later on, an accumulation of events with similar characteristics in the $\pi^+\pi^- J/\psi$, $\pi^0\pi^0 J/\psi$ and the $K^+K^- J/\psi$ mass spectra was reported by the CLEO collaboration [104,105], thus confirming the results from BABAR. Following these works, the BELLE collaboration obtained the cross sections for the $e^+e^- \rightarrow \pi^+\pi^- J/\psi$ reaction in the 3.8 to 5.5 GeV region [106], by keeping all the interactions in the final state in S -wave, and found a peak at 4.26 GeV and a bump around 4.05 GeV.

Although the $Y(4260)$ does not seem to fit in to the charmonium spectrum of the particle data group [71] known up to ~ 4.4 GeV, a proposal to accommodate it as a $4s$ state has been made in [107]. Several other suggestions have been made for the interpretation of this state, for example, the authors of [108] propose it to be a tetra-quark state, others propose a hadronic molecule of $D_1 D$, $D_0 D^*$ [109,110], $\chi_{c1}\omega$ [111], $\chi_{c1}\rho$ [112] and yet another idea is that it is a hybrid charmonium [113] or charm baryonium [114], etc. Within the available experimental information, none of these suggestions can be completely ruled out and its not clear if $Y(4260)$ possesses any of these structures dominantly or is a mixture of all of them. In Refs. [115,116,117] the authors call the attention of the readers to the presence of the opening of the $D_s^* \bar{D}_s^*$ channel very close to the peak position of the $Y(4260)$ in the updated data from BABAR [118] and associate the peak corresponding to $Y(4260)$ to a

$D_s^* \bar{D}_s^*$ cusp. A fit to the data from [103,118] has been made in [116] and the presence of a rather broad bump around 4.35 GeV has been proposed.

There are some peculiarities in the experimental findings which motivate us to carry out a study of the $J/\psi\pi\pi$ system. There is no enhancement found around 4.26 GeV in the process with the $D^* \bar{D}^*$ [119] or other hadron final states [120] and it is concluded that $Y(4260)$ has an unusually strong coupling to the $\pi\pi J/\psi$ final state [103,104,105,106]. Further, the data on the invariant mass of the $\pi\pi$ subsystem obtained by the Belle collaboration [106], for total energy range, 3.8-4.2 GeV, 4.2-4.4 GeV and 4.4-4.6 GeV, have curious features. The $\pi\pi$ mass distribution data in 3.8-4.2 GeV and 4.4-4.6 GeV seem to follow the phase space, however, that corresponding to the 4.2-4.4 GeV total energy differs significantly from the phase space and shows an enhancement near $m_{\pi\pi} = 1$ GeV. Do these findings indicate that the $Y(4260)$ has a strong coupling to $f_0(980)J/\psi$, similar to the $X(2175)$ to the $\phi f_0(980)$ [121,122]. It is interesting to recall that the $X(2175)$ was found as a dynamically generated resonance in the $\phi K\bar{K}$ system [96,123] with the $K\bar{K}$ subsystem possessing the characteristics of the $f_0(980)$. Similarly, the $Y(4660)$ [124] has been suggested as a $\psi' f_0(980)$ resonance [125]. In order to find an answer to this question, in [126] the Faddeev equations were solved for the $J/\psi\pi\pi$ and $J/\psi K\bar{K}$ coupled channels and the results are shown in fig. 10, where one sees that a peak of the amplitude squared is generated around an energy of 4150 MeV and \sqrt{s}_{23} around 980 MeV.

12 Conclusions

There have been several topics addressed in this talk around kaonic clusters, some of them involving kaons and nucleons or kaons and vector mesons. The conclusions have been appearing in each of the sections. As a brief summary we can conclude that antikaons are very peculiar particles, with very strong interaction with nucleons and mesons, either pseudoscalar or vectors. They provide a glue to bind many systems, however, some of them, particularly those involving several nucleons, seem to decay faster than we could observe. Yet, we found some other systems which are long lived enough, or sufficiently separated from other related states, such that their observation is possible and many of them have already been observed. We also think this is just the beginning in the search for these kind of new states and anticipate that many more states, of three body nature, or even with more particles, will eventually be seen in the future. Devoting work to this issue at the present time seems to us a very good scientific investment.

References

1. G. Ecker, Prog. Part. Nucl. Phys. **35**, 1 (1995) [arXiv:hep-ph/9501357].
2. V. Bernard, N. Kaiser and U. G. Meissner, Int. J. Mod. Phys. E **4**, 193 (1995) [arXiv:hep-ph/9501384].

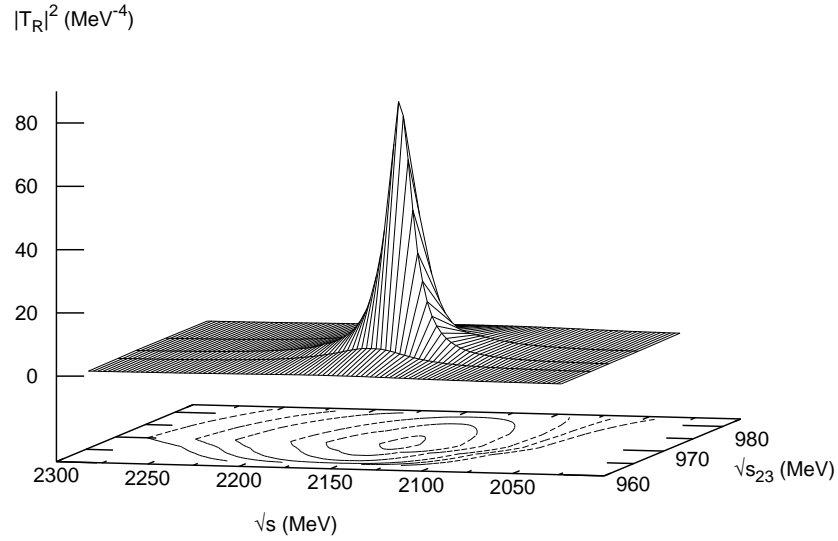


Figure 9. The $\phi K \bar{K}$ squared amplitude in the isospin 0 configuration.

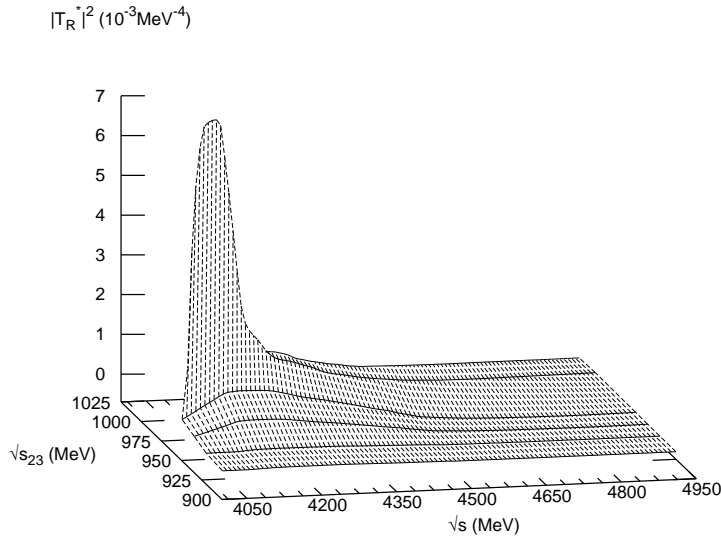


Figure 10. $|T_R^*|^2$ for the $J/\psi K \bar{K}$ system in total isospin $I = 0$ as a function of the total energy, \sqrt{s} , and the invariant mass of the $K \bar{K}$ subsystem, $\sqrt{s_{23}}$.

3. E. Oset and A. Ramos, Nucl. Phys. A **635**, 99 (1998) [arXiv:nucl-th/9711022].
4. J. A. Oller and E. Oset, Nucl. Phys. A **620** 438 (1997) [Erratum-ibid. A **652** 407 (1999)].
5. D. Gamermann, J. Nieves, E. Oset and E. R. Arriola, arXiv:0911.4407 [hep-ph].
6. V. Koch, Phys. Lett. B **337** (1994) 7
7. T. Waas, N. Kaiser and W. Weise, Phys. Lett. B **365** (1996) 12; *ibid.* B **379** (1996) 34
8. T. Waas and W. Weise, Nucl. Phys. A **625** (1997) 287
9. M. Lutz, Phys. Lett. B **426** (1998) 12
10. A. Ramos and E. Oset, Nucl. Phys. A **671** (2000) 481 [arXiv:nucl-th/9906016].

11. J. Schaffner-Bielich, V. Koch and M. Effenberger, Nucl. Phys. A **669** (2000) 153 [arXiv:nucl-th/9907095].
12. A. Cieply, E. Friedman, A. Gal and J. Mares, Nucl. Phys. A **696** (2001) 173 [arXiv:nucl-th/0104087].
13. L. Tolos, A. Ramos and E. Oset, Phys. Rev. C **74** (2006) 015203 [arXiv:nucl-th/0603033].
14. S. Hirenzaki, Y. Okumura, H. Toki, E. Oset and A. Ramos, Phys. Rev. C **61** (2000) 055205.
15. A. Baca, C. Garcia-Recio and J. Nieves, Nucl. Phys. A **673** (2000) 335 [arXiv:nucl-th/0001060].
16. R. S. Hayano *et al.* [KEK-E570 Collaboration], Mod. Phys. Lett. A **23**, 2505 (2008).
17. Y. Akaishi and T. Yamazaki, Phys. Rev. C **65** (2002) 044005.
18. Y. Akaishi, A. Dote and T. Yamazaki, Phys. Lett. B **613** (2005) 140 [arXiv:nucl-th/0501040].
19. E. Friedman, A. Gal, and C. J. Batty, Nucl. Phys. A **579** (1994) 518
20. D. B. Kaplan and A. E. Nelson, Phys. Lett. B **175** (1986) 57.
21. E. Friedman, A. Gal and J. Mares, Phys. Rev. C **60** (1999) 024314 [arXiv:nucl-th/9804072].
22. J. Mares, E. Friedman and A. Gal, Phys. Lett. B **606** (2005) 295 [arXiv:nucl-th/0407063].
23. J. Mares, E. Friedman and A. Gal, Nucl. Phys. A **770** (2006) 84 [arXiv:nucl-th/0601009].
24. D. Gazda, E. Friedman, A. Gal and J. Mares, Phys. Rev. C **76** (2007) 055204 [arXiv:0708.2157 [nucl-th]].
25. E. Friedman and A. Gal, Phys. Rept. **452** (2007) 89 [arXiv:0705.3965 [nucl-th]].
26. T. Muto, T. Maruyama and T. Tatsumi, Phys. Rev. C **79** (2009) 035207 [arXiv:0812.2537 [nucl-th]].
27. T. Maruyama, T. Tatsumi, T. Endo and S. Chiba, Recent Res. Devel. Physics 7 (2006) 1 [arXiv:nucl-th/0605075].
28. T. Maruyama, T. Tatsumi, D. N. Voskresensky, T. Tanigawa, T. Endo and S. Chiba, Phys. Rev. C **73** (2006) 035802 [arXiv:nucl-th/0505063].
29. X. H. Zhong, L. Li, C. H. Cai and P. Z. Ning, Commun. Theor. Phys. **41** (2004) 573.
30. X. H. Zhong, G. X. Peng, L. Li and P. Z. Ning, Phys. Rev. C **74** (2006) 034321.
31. L. Dang, L. Li, X. H. Zhong and P. Z. Ning, Phys. Rev. C **75** (2007) 068201 [arXiv:nucl-th/0701060].
32. E. Oset and H. Toki, Phys. Rev. C **74** (2006) 015207 [arXiv:nucl-th/0509048].
33. T. Hyodo and W. Weise, Phys. Rev. C **77**, 035204 (2008) [arXiv:0712.1613 [nucl-th]].
34. T. Yamazaki and Y. Akaishi, Nucl. Phys. A **792** (2007) 229 [arXiv:nucl-ex/0609041].
35. E. Oset, V. K. Magas, A. Ramos and H. Toki, proceedings of the IX International Conference on Hypernuclear and Strange Particle Physics, Mainz (Germany), October 10-14, 2006. Edited by J. Pochodzalla and Th. Walcher, (Springer, Germany, 2007), 263
36. A. Ramos, V. K. Magas, E. Oset and H. Toki, Nucl. Phys. A **804** (2008) 219.
37. N. V. Shevchenko, A. Gal, J. Mares Jose Goity wrote: and J. Revai, Phys. Rev. C **76**, 044004 (2007) [arXiv:0706.4393 [nucl-th]].
38. A. Dote, T. Hyodo and W. Weise, Nucl. Phys. A **804**, 197 (2008) [arXiv:0802.0238 [nucl-th]].
39. Y. Ikeda and T. Sato, Phys. Rev. C **76**, 035203 (2007) [arXiv:0704.1978 [nucl-th]].
40. T. Yamazaki and Y. Akaishi, Phys. Rev. C **76**, 045201 (2007) [arXiv:0709.0630 [nucl-th]].
41. T. Suzuki *et al.*, Phys. Lett. B **597** (2004) 263.
42. M. Agnello *et al.* [FINUDA Collaboration], Phys. Rev. Lett. **94** (2005) 212303.
43. M. Agnello *et al.* [FINUDA Collaboration], Phys. Lett. B **654** (2007) 80 [arXiv:0708.3614 [nucl-ex]].
44. V. K. Magas, E. Oset, A. Ramos and H. Toki, Phys. Rev. C **74** (2006) 025206 [arXiv:nucl-th/0601013];
45. V. K. Magas, E. Oset, A. Ramos and H. Toki, [arXiv:nucl-th/0611098].
46. V. K. Magas, E. Oset and A. Ramos, Phys. Rev. C **77**, 065210 (2008) [arXiv:0801.4504 [nucl-th]]; [arXiv:0901.1086 [nucl-th]];
47. T. Suzuki *et al.* [KEK-PS E549 Collaboration], Phys. Rev. C **76** (2007) 068202 [arXiv:0709.0996 [nucl-ex]].
48. T. Kishimoto *et al.*, Prog. Theor. Phys. **118**, 181 (2007).
49. V. K. Magas, J. Yamagata-Sekihara, S. Hirenzaki, E. Oset, A. Ramos, arXiv:0911.3614 [nucl-th]; arXiv:0911.2091 [nucl-th]; A. Ramos, V. K. Magas, J. Yamagata-Sekihara, S. Hirenzaki, E. Oset, arXiv:0911.4841 [nucl-th].
50. O. Morimatsu and K. Yazaki, Prog. Part. Nucl. Phys. **33**, 679 (1994).
51. J. Yamagata and S. Hirenzaki, Eur. Phys. J. **A31**, 255 (2007).
52. J. Yamagata, H. Nagahiro, R. Kimura and S. Hirenzaki, Phys. Rev. C **76**, 045204 (2007) [arXiv:0708.0459 [nucl-th]].
53. J. Yamagata-Sekihara, D. Jido, H. Nagahiro and S. Hirenzaki, Phys. Rev. C **80**, 045204 (2009) [arXiv:0812.4359 [nucl-th]].
54. P. A. Katz, K. Bunnell, M. Derrick, T. Fields, L. G. Hyman and G. Keyes, Phys. Rev. D **1** (1970) 1267.
55. E. Oset, Y. Futami and H. Toki, Nucl. Phys. A **448**, 597 (1986).
56. H. J. Weyer, Phys. Rept. **195** (1990) 295.
57. L. L. Salcedo, E. Oset, M. J. Vicente-Vacas and C. Garcia-Recio, Nucl. Phys. A **484**, 557 (1988).
58. T. S. Kosmas and E. Oset, Phys. Rev. C **53**, 1409 (1996).
59. C. Albertus, J. E. Amaro and J. Nieves, Phys. Rev. Lett. **89**, 032501 (2002) [arXiv:nucl-th/0110046].
60. J. Nieves, J. E. Amaro and M. Valverde, Phys. Rev. C **70**, 055503 (2004) [Erratum-ibid. C **72**, 019902 (2005)] [arXiv:nucl-th/0408005].
61. A. Ramos, V. K. Magas, E. Oset and H. Toki, Eur. Phys. J. **A31**, 684 (2007); [arXiv:nucl-th/0702019].
62. A. Doté and W. Weise, Prog. Theor. Phys. Suppl. **168**, 593 (2007); A. Doté and W. Weise, nucl-th/0701050, in: Proceedings HYP06, "Hypernuclear and Strange Particle Physics", J. Pochodzalla and Th. Walcher,

- ed., p 249, Springer, Heidelberg, 2007 (ISBN 978-3-540-76365-9).
63. A. Arai, M. Oka and S. Yasui, *Prog. Theor. Phys.* **119**, 103 (2008).
 64. T. Koike and T. Harada, *Phys. Lett.* **B652**, 262 (2007); *Nucl. Phys.* **A804**, 231 (2008).
 65. R. H. Dalitz, T. C. Wong and G. Rajasekaran, *Phys. Rev.* **153** (1967) 1617.
 66. P. B. Siegel and W. Weise, *Phys. Rev. C* **38**, 2221 (1988).
 67. D. Jido, J. A. Oller, E. Oset, A. Ramos and U. G. Meissner, *Nucl. Phys. A* **725**, 181 (2003) [arXiv:nucl-th/0303062].
 68. D. W. Thomas, A. Engler, H. E. Fisk and R. W. Kraemer, *Nucl. Phys. B* **56** (1973) 15.
 69. A. Martinez Torres, K. P. Khemchandani and E. Oset, *Phys. Rev. C* **77**, 042203 (2008).
 70. A. Martinez Torres, K. P. Khemchandani and E. Oset, *Eur. Phys. J. A* **35**, 295 (2008) [arXiv:0805.3641 [nucl-th]].
 71. C. Amsler *et al.* [Particle Data Group], *Phys. Lett. B* **667**, 1 (2008).
 72. D. Jido and Y. Kanada-En'yo, *Phys. Rev. C* **78**, 035203 (2008) [arXiv:0806.3601 [nucl-th]].
 73. A. Martinez Torres, K. P. Khemchandani and E. Oset, arXiv:0812.2235 [nucl-th].
 74. T. Inoue, E. Oset and M. J. Vicente Vacas, *Phys. Rev. C* **65**, 035204 (2002) [arXiv:hep-ph/0110333].
 75. A. Martinez Torres, K. P. Khemchandani, U. G. Meissner and E. Oset, *Eur. Phys. J. A* **41**, 361 (2009) [arXiv:0902.3633 [nucl-th]].
 76. R. Bradford *et al.* [CLAS Collaboration], *Phys. Rev. C* **73**, 035202 (2006) [arXiv:nucl-ex/0509033].
 77. F. X. Lee, T. Mart, C. Bennhold and L. E. Wright, *Nucl. Phys. A* **695**, 237 (2001) [arXiv:nucl-th/9907119].
 78. B. Borasoy, P. C. Bruns, U. G. Meissner and R. Nissler, *Eur. Phys. J. A* **34**, 161 (2007) [arXiv:0709.3181 [nucl-th]].
 79. V. Bernard, N. Kaiser and U.-G. Meißner, *Int. J. Mod. Phys. E* **4**, 193 (1995) [arXiv:hep-ph/9501384].
 80. F. E. Close and R. G. Roberts, *Phys. Lett. B* **316**, 165 (1993) [arXiv:hep-ph/9306289].
 81. E. Oset and A. Ramos, *Nucl. Phys. A* **679**, 616 (2001) [arXiv:nucl-th/0005046].
 82. V. A. Nikonov, A. V. Anisovich, E. Klempt, A. V. Sarantsev and U. Thoma, *Phys. Lett. B* **662**, 245 (2008) [arXiv:0707.3600 [hep-ph]].
 83. D. Drechsel, *Prog. Part. Nucl. Phys.* **34**, 181 (1995) [arXiv:nucl-th/9411034].
 84. J. Ahrens *et al.* [GDH Collaboration and A2 Collaboration], *Phys. Rev. Lett.* **87**, 022003 (2001) [arXiv:hep-ex/0105089].
 85. J. Ahrens *et al.* [GDH and A2 Collaborations], *Eur. Phys. J. A* **34**, 11 (2007).
 86. J. C. Nacher and E. Oset, *Nucl. Phys. A* **697**, 372 (2002) [arXiv:nucl-th/0106005].
 87. T. Nakano, private communication.
 88. B. Aubert *et al.* *Phys. Rev. D* **74** 091103 (2006).
 89. B. Aubert *et al.* *Phys. Rev. D* **76** 012008 (2007).
 90. M. Ablikim *et al.* [BES Collaboration], *Phys. Rev. Lett.* **100**, 102003 (2008).
 91. Z. G. Wang, *Nucl. Phys. A* **791** 106 (2007).
 92. G. J. Ding and M. L. Yan, *Phys. Lett. B* **657** 49 (2007).
 93. F. E. Close, arXiv:0706.2709 [hep-ph].
 94. S. L. Zhu, *Int. J. Mod. Phys. E* **17**, 283 (2008).
 95. *Phys. Rev. D* **76** 074012 (2007).
 96. A. Martinez Torres, K. P. Khemchandani, L. S. Geng, M. Napsuciale and E. Oset, *Phys. Rev. D* **78**, 074031 (2008) [arXiv:0801.3635 [nucl-th]].
 97. N. Kaiser, *Eur. Phys. J. A* **3** 307 (1998).
 98. V. E. Markushin, *Eur. Phys. J. A Meissner* **8** 389 (2000).
 99. M. F. M. Lutz and E. E. Kolomeitsev, *Nucl. Phys. A* **730**, 392 (2004).
 100. L. Roca, E. Oset and J. Singh, *Phys. Rev. D* **72** 014002 (2005).
 101. A. Martinez Torres, K. P. Khemchandani and E. Oset, *Phys. Rev. C* **77**, 042203 (2008).
 102. K. P. Khemchandani, A. Martinez Torres and E. Oset, *Eur. Phys. J. A* **37**, 233 (2008) [arXiv:0804.4670 [nucl-th]].
 103. B. Aubert *et al.* [BABAR Collaboration], *Phys. Rev. Lett.* **95** 142001(2005).
 104. T. E. Coan *et al.* [CLEO Collaboration], *Phys. Rev. Lett.* **96**, 162003 (2006).
 105. Q. He *et al.* [CLEO Collaboration], *Phys. Rev. D* **74**, 091104 (2006).
 106. C. Z. Yuan *et al.* [Belle Collaboration], *Phys. Rev. Lett.* **99**, 182004 (2007).
 107. F. J. Llanes-Estrada, *Phys. Rev. D* **72**, 031503 (2005).
 108. L. Maiani, V. Riquer, F. Piccinini and A. D. Polosa, *Phys. Rev. D* **72**, 031502 (2005).
 109. G. J. Ding, *Phys. Rev. D* **79**, 014001 (2009).
 110. R. M. Albuquerque and M. Nielsen, *Nucl. Phys. A* **815**, 53 (2009).
 111. C. Z. Yuan, P. Wang and X. H. Mo, *Phys. Lett. B* **634**, 399 (2006).
 112. X. Liu, X. Q. Zeng and X. Q. Li, *Phys. Rev. D* **72**, 054023 (2005).
 113. S. L. Zhu, *Phys. Lett. B* **625**, 212 (2005).
 114. C. F. Qiao, *Phys. Lett. B* **639**, 263 (2006).
 115. E. van Beveren and G. Rupp, arXiv:hep-ph/0605317.
 116. E. van Beveren and G. Rupp, arXiv:0904.4351 [hep-ph].
 117. E. van Beveren and G. Rupp, arXiv:0905.1595 [hep-ph].
 118. B. Aubert *et al.* [BaBar Collaboration], arXiv:0808.1543 [hep-ex].
 119. B. Aubert *et al.* [BABAR Collaboration], arXiv:0903.1597 [hep-ex].
 120. S. Eidelman *et al.* [Particle Data Group], *Phys. Lett. B* **592**, 1 (2004).
 121. B. Aubert *et al.* [BABAR Collaboration], *Phys. Rev. D* **74**, 091103 (2006).
 122. M. Ablikim *et al.* [BES Collaboration], *Phys. Rev. Lett.* **100**, 102003 (2008).
 123. L. Alvarez-Ruso, J. A. Oller and J. M. Alarcon, *Phys. Rev. D* **80**, 054011 (2009) [arXiv:0906.0222 [hep-ph]].

124. X. L. Wang *et al.* [Belle Collaboration], Phys. Rev. Lett. **99**, 142002 (2007) .
125. F. K. Guo, C. Hanhart and U. G. Meissner, Phys. Lett. B **665**, 26 (2008).
126. A. Martinez Torres, K. P. Khemchandani, D. Gamermann and E. Oset, Phys. Rev. D **80**, 094012 (2009) [arXiv:0906.5333 [nucl-th]].